Solar-Terrestrial Physics. 2024. Vol. 10. Iss. 3. P. 97–107. DOI: 10.12737/stp-103202412. © 2024 A.V. Moiseev, V.I. Popov, S.A. Starodubtsev. Published by INFRA-M Academic Publishing House

UDC 550.385.37
DOI: 10.12737/stp-103202412

Received March 30, 2024
Accepted May 13, 2024

INVESTIGATING AZIMUTHAL PROPAGATION OF Pc5 GEOMAGNETIC PULSATIONS AND THEIR EQUIVALENT CURRENT VORTICES FROM GROUND-BASED AND SATELLITE DATA

A.V. Moiseev
Yu.G. Shafer Institute of Cosmophysical Research and Aeronomy SB RAS, Yakutsk, Russia, moiseev@ikfia.ysn.ru

V.I. Popov
Yu.G. Shafer Institute of Cosmophysical Research and Aeronomy SB RAS, Yakutsk, Russia, volts@mail.ru

S.A. Starodubtsev
Yu.G. Shafer Institute of Cosmophysical Research and Aeronomy SB RAS, Yakutsk, Russia, starodub@ikfia.ysn.ru

Abstract. Using phase delays at spaced stations and satellite observations in the magnetosphere during two events, we have studied azimuthal propagation of resonant bursts of geomagnetic pulsations in the Pc5 range. We have also examined propagation of equivalent current vortices during these events. It has been found that the pulsations, observed in the magnetosphere and ionosphere, and the equivalent current vortices in the ionosphere propagate in the azimuthal direction from the dayside to the nightside. Propagation velocities according to ground-based observations are 5–25 km/s; according to satellite observations, 114–236 km/s. Propagation velocities according to satellite observations do not exceed the Alfvén velocity in the magnetosphere, which is 620–1006 km/s. According to data from various instruments, there are signatures of fast magnetosonic and Alfvén waves at a time in one of the events on the satellite. This clearly reflects the transformation of these waves. The geomagnetic latitude of registration of vortex centers coincides with the latitude of the maximum amplitude of geomagnetic pulsations (field line resonances) and decreases by ~15° toward the early hours of MLT. The observed dynamics of Pc5 pulsations and vortices is assumed to reflect MHD wave propagation in the magnetosphere.

Keywords: geomagnetic Pc5 pulsations, equivalent current vortices, azimuthal propagation, wave disturbances in plasma parameters and geomagnetic field in Pc5 pulsations in the magnetosphere

INTRODUCTION

Ultra-low frequency (ULF) waves in the Pc5 range are known to play an important role in the magnetosphere dynamics [Saito, 1978]. The ULF waves generated at the boundary of the magnetosphere or in the solar wind (SW) transfer energy to the inner magnetosphere, where resonance eigenoscillations (field line resonance, FLR) are excited. The sources of FLR are considered to be modes of the magnetospheric cavity (waveguide) excited by SW dynamic pressure pulses P_d [Allan et al., 1986; Wright, 1994; Chelpanov et al., 2022] or by the Kelvin—Helmholtz instability on the flanks of the magnetosphere [Southwood, 1974; Chen, Hasegawa, 1974; Mishin, Matyukhin, 1986; Mann et al., 2002].

Under the Themis project, data from synchronous satellite and ground-based observations became available, offering the possibility to study types of ULF waves excited in the magnetospheric-ionospheric system, as well as to determine their direction and propagation velocity [Zhang et al., 2022]. A source of ULF waves is spatio-temporal variations in the intensity of three-dimensional current systems [Saito, 1969; Motoba et al., 2002]. Traveling convection vortices (TCVs) are a special case of ULF wave current systems [Friis-Christensen et al., 1988; Glassmeier, 1992]. A source of TCVs is considered to be a local effect on the dayside magnetopause [Korotova et al., 2004] due to P_d pulses or impulsive reconnection at the magnetopause — flux transfer event (FTE). TCVs propagate mainly to the west along the azimuth in the dawn sector, but, as shown in the statistical study [Zesta et al., 2002], they can also propagate to the east. The TCV study based on spherical elementary current systems (the method used in this study) has been carried out in [Amm et al., 2002]: the authors have estimated the propagation velocity and direction of a pair of TCVs, densities of equivalent ionospheric and field-aligned currents. Chinkin et al. [2020] have examined the dynamics of TCVs, using the method they developed for calculating equivalent ionospheric currents (EICs). Propagation of TCVs has been investigated from phase delays of magnetic pulses in [Friis-Christensen et al., 1988; Lühr et al., 1996]. Yet, we do not know any works comparing azimuthal velocities of TCV propagation obtained both from phase delays of magnetic impulses and from the displacement of vortex centers.

The purpose of this work is to compare propagation of geomagnetic Pc5 pulsations and centers of EIC vortices, excited during these pulsations in the azimuthal direction, using ground and satellite observations. For

the analysis, we have selected two events of bursts of Pc5 geomagnetic pulsations occurring on February 15, 2011 and January 12, 2008.

1. EXPERIMENTAL DATA

To study azimuthal propagation of Pc5 geomagnetic pulsations and equivalent current vortices, we have used geomagnetic observations from the well-known SUPERMAG database [Gjerloev, 2012; http://supermag.jhuapl.edu/mag]. Coordinates of the stations employed to examine propagation of Pc5 pulsations and equivalent current vortices are listed in Table 1 and 2 respectively. Measurements by THEMIS satellites have been taken from the CDAWEB database [http://cdaweb.gsfc.nasa.gov]. Coordinates of the satellites in the magnetosphere are given in Table 3. To study propagation, we have used data from ground-based station with a time resolution of 60 s since the distance between the stations in azimuth was >500 km, and the duration of phase delays of signals was ≥60 s. The time resolution of the satellite data was 3 s.

2. ANALYSIS METHOD

In this paper, we compare azimuthal propagation velocities obtained by two methods: from phase delays of magnetic variations at stations (method 1) and from the movement of EIC vortices (method 2).

The location of the global network stations made it possible to analyze azimuthal propagation along geomagnetic latitudes 57°–60°, 65°–66°, and 68°–71°.

Calculations by both methods were made in Matlab. In this case, method 1 involves applying the function findpeaks [https://www.mathworks.com/help/signal/ref/findpeaks.html] to the interval of the data filtered in the Pc5 range (T=150–600 s). With this function we determined the time of detection of the characteristic maximum of signals, received from neighboring stations, in the time interval processed, and estimated the phase shift between them. By determining the distance between the longitudinally spaced stations by the method described in [Makarov et al., 2002], and knowing the phase delay of pulsations between them, we can find propagation velocities.

Method 2 can construct two-dimensional spherical elementary current systems describing the equivalent current density on a computational grid [Vanhamäki, Juusola, 2020]. The disturbance of the geomagnetic field is described by superposing the magnetic field of divergence-free ionospheric elementary current systems. From amplitudes of these systems, we determine EICs. The method allows us to analyze the distribution of currents on the intervals of observation of Pc5 pulsations and to estimate the location of EIC vortices. The distances between their locations and propagation velocities were determined from geomagnetic coordinates of vortex centers in latitude and longitude every 60 s.

The vortex velocities thus determined were compared with the propagation velocities of Pc5 geomagnetic pulsations.

The dynamics of EIC vortices is analyzed using the program code, written in Matlab, from [Vanhamäki, Juusola, 2020] available at [https://link.springer.com/chapter/10.1007/978-3-030-26732-2_2#Sec18]. The vortex center, as in [Chinkin et al., 2020], was found from extremums of the function

$$\mathbf{G}(x, y)=\mathrm{rot}(\mathbf{J}/|\mathbf{J}|), \quad (1)$$

where J is the horizontal ionospheric current.

Method 1 allows us to estimate phase velocities of pulsation propagation; method 2, group velocities of vortex propagation.

To identify Pc5 pulsations from geomagnetic data, we have used the digital bandpass filter detailed in [Hemming, 1980],

$$y_n = \sum_{k=-M}^{M} c_k x_{n-k}. \quad (2)$$

Here, c_k denotes filter coefficients; k is the number of filter coefficients; x designates values of the initial implementation; y indicates the values obtained by filtration; n is the number of measurements; M is the specified maximum number of filter coefficients. The coefficients of the filter c_k are related to its amplitude-frequency response $H(\omega)$ by the inverse Fourier transform:

$$c_k = \frac{1}{2\pi}\int_{-\pi}^{\pi} H(\omega)\exp(j\omega k)\,d\omega, \quad \omega = 2\pi\nu,\ j=\sqrt{-1} \quad (3)$$

for the frequencies $\nu_1 < \nu < \nu_2 = 1/(2\Delta t)$, Δt is the sampling interval of data; $\omega = 2\pi\nu$.

The filter coefficients were selected in such a way that the bandwidth of the amplitude-frequency response corresponded to the periods of Pc5 pulsations in the range of 150 to 600 s and pulsations on the filter plateau did not exceed 1 %.

3. ANALYSIS RESULTS

Figure 1 presents measurements of parameters of plasma (ion concentration and velocity, *a*–*d*) and magnetic field in the magnetosphere (*e*–*h*) from the THEMIS D, E, A (ThD, ThE, ThA) satellites in the February 15, 2011 event. Plasma and magnetic field parameters from different satellites are shown by different colors and hatching. At the bottom (*i*) are variations in the *H* component obtained at the ground-based stations located in the field line projection of these satellites. In this event, ~6 min pulsations on Earth are seen to begin at 06:54–06:56 UT (*i*). Concurrent pulsations in the magnetic field and the ion velocities recorded by the satellites, located on the nightside near the geostationary orbit, began at about the same time (*b*–*h*).

Signal phase delays at ground-based stations and different satellites corresponded to propagation toward the magnetotail (in the antisolar direction). Since the pulsations in the velocity components are more regular than the pulsations in the magnetic field, we used them to determine signal phase delays. We employed magnetic field variations to study pulsation polarization. Pulsations from satellite and ground-based observations looked about the same in the January 12, 2008 event. Note that the Pc5 pulsations in the interval of interest were recorded locally in the 00:00–12:00 MLT sector (from midnight to noon).

Table 1

Coordinates of ground-based stations (SMAG) used to study azimuthal propagation of pulsations

Averaged latitude	Abbreviation	Geographic coordinates		Corrected geomagnetic coordinates	
		latitude	longitude	latitude	longitude
68–71	BJN	74.50	19.20	71.89	107.71
	SCO	70.48	338.03	71.63	71.82
	SKT	65.42	307.1	71.43	37.22
	CDC	64.2	283.4	73.47	3.04
	INK	68.25	226.7	71.5	–83.05
	BRW	71.3	203.25	70.6	–106.57
	GHB	62.00	310.32	67.41	39.05
	IQA	63.75	291.48	72.21	15.58
	FCC	58.76	265.92	68.5	–25.57
	YKS	62.48	245.52	69.42	–56.85
	DED	211.21	211.21	70.87	–99.27
65–67	MAS	69.46	23.70	66.65	106.36
	KEV	69.76	27.01	66.82	109.22
	TRO	69.66	18.94	67.07	102.77
	AND	69.30	16.03	66.86	100.22
	LRV	64.18	338.30	65.01	66.72
	NAQ	61.16	314.56	65.75	43.19
	T29	58.10	291.60	66.70	14.25
	T31	56.50	280.80	66.31	–1.92
	GIM	56.38	265.36	66.16	–26.08
	RAL	58.22	256.32	67	–40.08
	FSP	61.76	238.77	67.47	–64.89
57–60	MEK	62.77	30.97	59.57	108.66
	SOL	61.08	4.84	58.82	86.25
	LER	60.13	358.82	58.20	80.96
	OUJ	64.52	27.23	61.47	106.27
	LYC	64.61	18.75	61.87	99.33
	RVK	64.94	10.99	62.61	93.27
	T28	53.3	299.5	60.49	23.61
	T32	49.40	277.70	59.52	–6.97
	PIN	50.2	263.96	59.96	–27.43
	MEA	54.62	246.65	61.85	–52.1
	C12	49.69	256.20	58.49	–38.32
	RED	52.14	246.16	59.25	–51.96
	T37	53.8	237.2	59.16	–63.14
	T22	56.83	226.84	60.09	–75.54

To visually explain the pattern of propagation of Pc5 pulsations, Figure 2 shows the azimuthal profile of the *H* component at 65°–66° magnetic latitudes in the February 15, 2011 event. The stations are arranged in order of decreasing geomagnetic longitude from east to west. The data is filtered in the Pc5 range. The maxima selected to determine the phases delays are marked with asterisks, next to which are the delay values in seconds. Propagation is seen to be westward.

Figure 3 illustrates EIC distribution at the selected stations: Im (*a*), Gr (*b*), USA E-Gr (*c*), USA C-E (*d*), USA W-C (*e*). The stations for the analysis of azimuthal dynamics of vortices have been selected to provide two-dimensional coverage. It can be seen that the vortices moved mainly along the azimuth westward, but in the USA C-E (*d*) network the vortex shifted in a northeasterly direction.

Vortex shift in longitude was ~10°. Figure 4 illustrates the distribution of azimuthal propagation velocities of geomagnetic pulsations and centers of equivalent current vortices by MLT (geomagnetic longitude) in the February 15, 2011 (*a*) and January 12, 2008 (*b*) events. Panels *c*, *d* show the distribution of geomagnetic latitudes of centers of equivalent current vortices, as well as field line resonances relative to MLT in the February 15, 2011 (*c*) and January 12, 2008 (*d*) events. Propagation of pulsations was studied along 57°–60°, 65°–66°, and 68°–71° latitude ranges, and propagation of vortices was analyzed relative to the selected stations providing two-dimensional coverage. Also shown are measurement errors calculated from instrumental measurement errors of the physical parameters used with a confidence level of 95 %. Positive velocities correspond to westward propagation; negative ones, to eastward propagation. Westward propagation of both Pc5 pulsations and vortices is seen (panels *a*, *b*) to prevail in both events, which exhibit an increase in velocity from 5–10 to 20–25 km/s in the 04–06 MLT sector, and then its decrease to the initial value, well pronounced on February 15, 2011.

Table 2

Coordinates of ground-based magnetometric stations,
used to study the dynamics of vortices of equivalent ionospheric currents

Abbreviation	Network	Geographic coordinates		Corrected geographic coordinates	
		latitude	longitude	latitude	longitude
NAL	Im	78.92	11.95	76.57	109.96
LYR		78.20	15.83	75.64	111.03
HOR		77.00	15.60	74.52	108.72
SOR		70.54	22.22	67.8	106.04
HOP		76.51	25.01	73.53	114.59
BJN		74.50	19.20	71.89	107.71
NOR		71.09	25.79	68.19	109.28
SOR*		70.54	22.22	67.80	106.04
KEV		69.76	27.01	66.82	109.22
IVA		68.56	27.29	65.60	108.61
MUO		68.02	23.53	65.19	105.23
SOD		67.37	26.63	64.41	107.33
THL	Gr	77.47	290.77	84.72	29.24
SVS		76.02	294.9	83	32.87
KUV		74.57	302.82	80.69	41.92
UPN		72.78	303.85	78.93	40.20
UMQ		70.68	307.87	76.38	42.58
GDH		69.25	306.47	75.25	39.39
ATU		67.93	306.43	73.99	38.19
STF		67.02	309.28	72.64	40.87
SKT		65.42	307.10	71.43	37.22
GHB		64.17	308.27	69.98	37.85
FHB		62.00	310.32	67.41	39.05
NAQ		61.16	314.56	65.75	43.19
RES	USA E-Gr	74.69	265.11	82.93	–35.54
TAL		69.54	266.45	78.51	–27.95
GHC		68.6	264.10	77.51	–31.76
BLC		64.33	263.97	73.61	–30.09
RAN		62.82	267.89	72.45	–23.12
FCC		58.76	265.92	68.5	–25.57
GIM		56.38	265.36	66.16	–26.08
ISL		53.86	265.34	63.70	–25.79
PIN		50.2	263.96	59.96	–27.43
CBB	USA C-E	69.1	255.00	77.04	–47.75
YKC		62.48	245.52	69.42	–56.85
SMI		60.02	248.05	67.47	–52.29
FMC		56.66	248.79	64.28	–50.02
MEA		54.62	246.65	61.85	–52.1
ROT		51.07	245.87	58.1	–52.01
C06		53.35	247.03	60.64	–51.24
RED		52.14	246.16	59.25	–51.96
LET		49.64	247.13	56.88	–50.07
NEW		48.27	242.88	54.65	–54.82
T19		47.61	245.33	54.45	–51.74
T25		45.14	241.07	51.06	–56.04
IGC	USA W-C	69.30	278.20	78.43	–5.39
CY0		70.5	291.4	78.52	18.88
RPB		66.50	273.80	75.99	–13.55
CDC		64.20	283.40	73.47	3.04
T29		58.10	291.60	66.70	14.25
T31		56.50	280.80	66.31	–1.92
T32		49.40	277.70	59.52	–6.97
T51		48.05	282.22	57.62	–0.74
OTT		45.40	284.45	54.81	2.25

Table 3

Coordinates of satellites in the magnetosphere in the GSM system for each event

№	Date	UT	Satellites	GSM coordinates, R_e		
				X	Y	Z
1	12.01.2008	08:00	Themis C	–7.05	–8.45	–2.26
			Themis D	–9.89	–5.32	–3.50
			Themis E	–9.97	–4.34	–3.60
2	15.02.2011	07:00	Themis D	–4.99	–4.41	–0.67
			Themis E	–5.13	–5.51	–0.74
			Themis A	–5.27	–6.03	–0.82

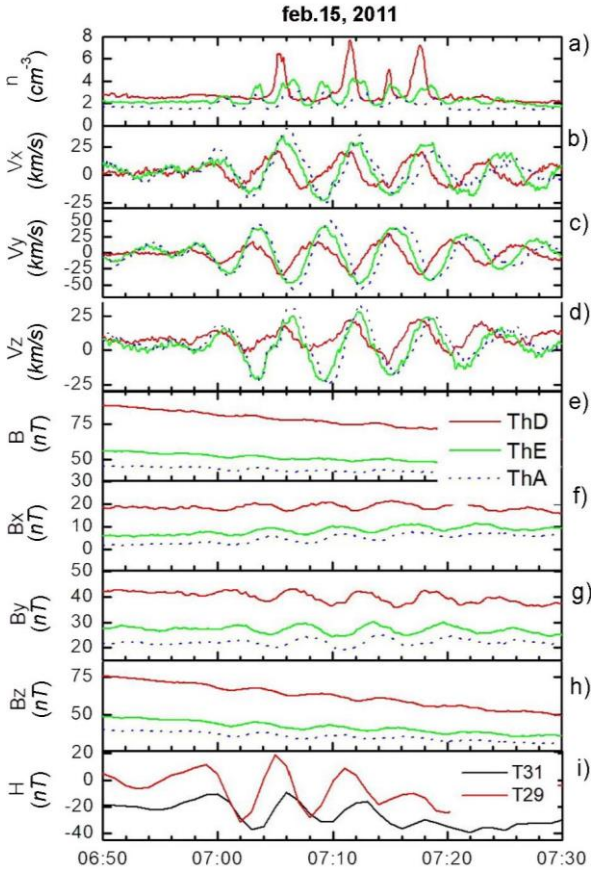

Figure 1. Medium parameters in the magnetosphere measured by THEMIS: ion concentration (*a*), V_x, V_y, V_z components of the ion velocity (*b–d*); B, B_x, B_y, B_z components of the geomagnetic field (*e–h*); variations in the geomagnetic field H component at ground-based stations (*i*)

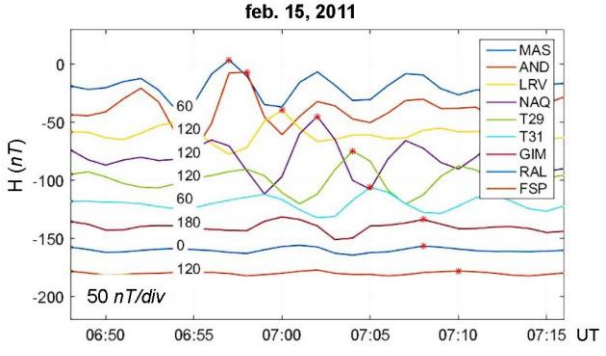

Figure 2. Azimuthal profiles of the geomagnetic field H component at 65°–66° magnetic latitudes in the February 15, 2011 event

It follows from the analysis that the azimuthal velocities of the vortex centers are generally consistent in magnitude and direction with the velocities of the geomagnetic pulsations. The velocities are 5–25 km/s, but for some vortices they exceed 36 km/s. The dynamics of the azimuthal velocity of TCVs in longitude in [Lühr et al., 1996] (2.5 km/s at 10:45 MLT followed by an increase to 7.4 km/s at 06:50 MLT) matches that we obtained. Velocities of two vortices in [Amm et al., 2002] were 7 and 3 km/s; in [Chinkin et al., 2020], 3.9 and 1.3 km/s with westward propagation, which also agrees with our results. Comparable azimuthal propagation velocities of 9.5 km/s at high latitudes were observed in [Dmitriev, Suvorova, 2023] when studying the magnetosheath jet shift from the noon sector to the dusk one. The latitude of centers of EIC vortices is seen (*c*, *d*) to linearly depend on MLT — it decreases by 10°–15° toward early hours (marked with vertical arrows). A similar dependence is also demonstrated by the latitudes at which the maximum amplitude of geomagnetic pulsations (field line resonance oscillations) is recorded, they coincide quite well with the latitudes of the centers of EIC vortices. The field line resonance oscillation latitudes are estimated from the amplitude and phase variations along the meridional profiles of magnetic stations located in regions where the dynamics of EIC vortices was examined (not shown). The resonance condition was considered to be the latitudinal maximum of pulsation amplitude, accompanied by a phase shift of ~180°, as proposed in [Glassmeier et al., 1999].

Figure 5 illustrates variations in the V_x component of the ion velocity from satellites (Th D, E, A) (*a*), time variations in magnetic field hodographs (B_x component is along the X-axis; B_y, along the Y-axis) obtained by the satellites (*b*); magnetic field hodographs from the ThD satellite (*c*) and ground-based station T31 (*d*) at 6:50–7:10 UT and 7:10–7:30 UT. The satellite and ground-based observations were filtered in the Pc5 range. Satellite data is given in the GSM coordinate system.

The phase delays in the oscillations between the ThD, ThE, and ThA satellites indicate wave propagation to the nightside. Phase propagation velocities between the satellites were calculated as the ratio of the distance between the satellites in the XY plane to the oscillation delay between them, V_{velD_E}=235.75, V_{velE_A}=114.49 km/s (V_{velC_D}=449.27 km/s in the January 12, 2008 event). Thus, the propagation velocities in the magnetosphere are 5–10 times higher than the maximum azimuthal propagation

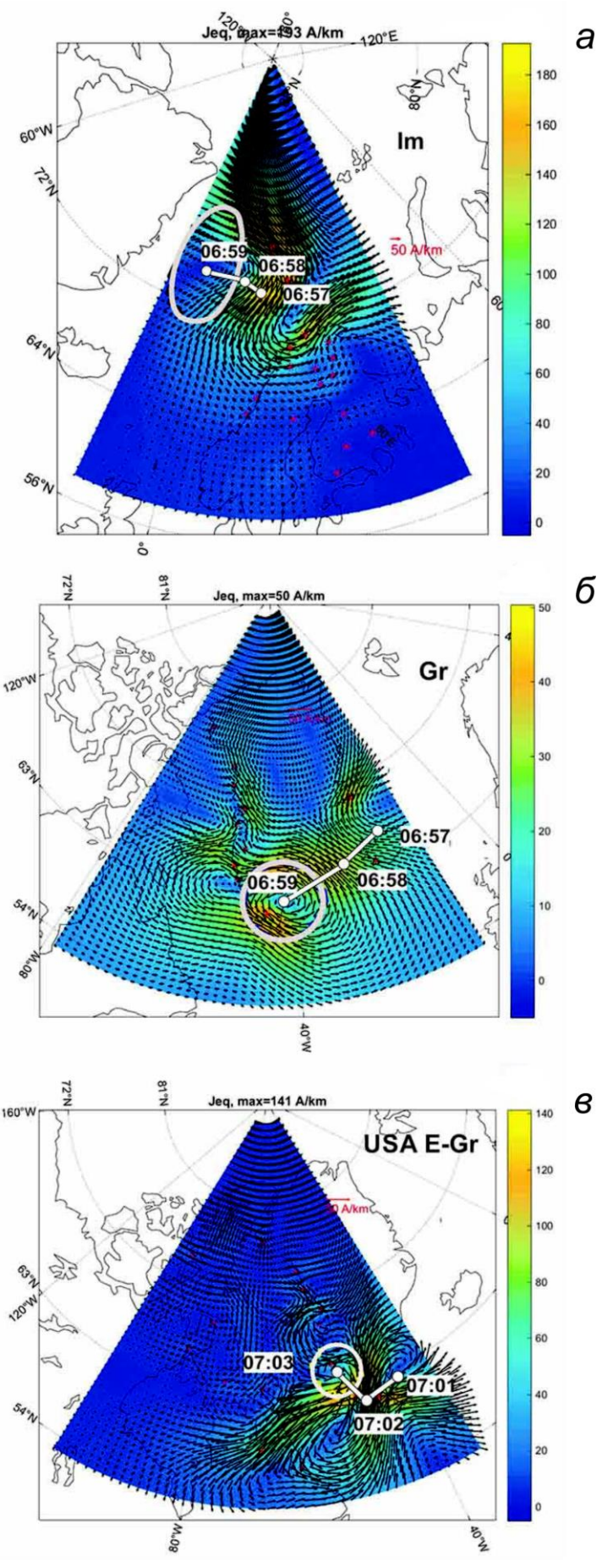
а
Jeq, max=193 A/km
Im
50 A/km
06:59
06:58
06:57
120°E
60°W
72°N
64°N
56°N
180
160
140
120
100
80
60
40
20
0
б
Jeq, max=50 A/km
Gr
06:57
06:59
06:58
120°W
63°N
54°N
80°W
40°W
50
40
30
20
10
0
в
Jeq, max=141 A/km
USA E-Gr
07:03
07:01
07:02
160°W
120°W
63°N
54°N
80°W
40°W
140
120
100
80
60
40
20
0

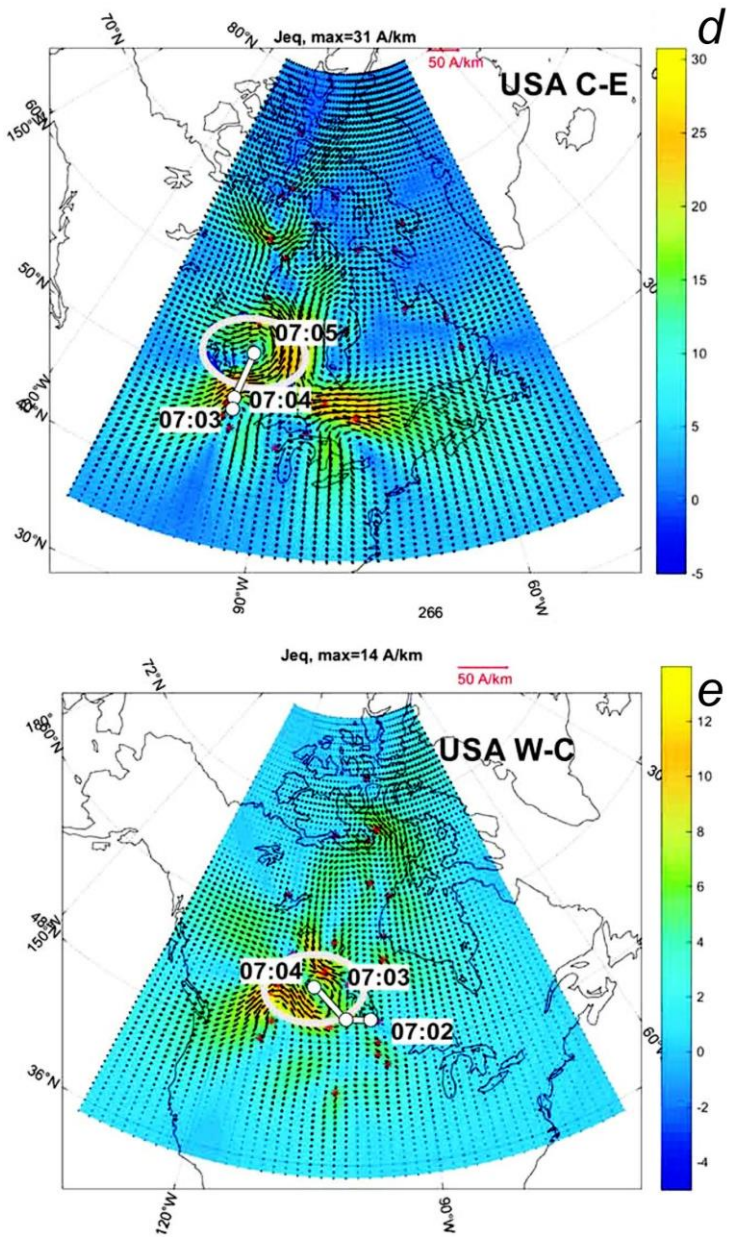

Figure 3. Distributions of equivalent ionospheric currents along arrays of stations Im (*a*) and Gr (*b*), USA E-Gr (*c*), USA C-E (*d*), USA W-C (*e*). The gray solid line is the vortex contour at the final moment of time; white lines in each panel indicate the trajectory of the vortex center shift in the time intervals indicated by numbers

velocity of 25 km/s according to ground observations, but do not exceed Alfvén velocities 620–1006 km/s in the magnetosphere.

The similarity between the oscillation hodographs obtained by different satellites (*b*) allows us to estimate phase delays in the resulting vector of oscillations of the magnetic field B_x and B_y components, $V_{MF\_D\_E}$=151, $V_{MF\_E\_A}$=79.5 km/s. The phase propagation velocities found from the ion velocity are comparable to the propagation velocities in the magnetic field. The phase velocities from satellites are close to the plasma flow velocity (usually ~100 km/s). In [Zhang et al., 2022], the phase velocity of propagation between satellites was ~400 km/s.

Comparison between polarizations of magnetic field vectors from the ThD satellite and ground station T31 (panels *b*, *d*) suggests that polarization of oscillations in the magnetosphere and ionosphere is elliptical, has the opposite direction, and tilts of the axes of the polarization ellipses are the same in both geospheres. The opposite direction of rotation is typical of Alfvén oscillations and corresponds to a 90° phase rotation. To compare the propagation velocities on Earth and in the magnetosphere, the ground stations located along 68°–71° magnetic latitudes were projected onto the equatorial plane of the magnetosphere, using the Tsyganenko model Ts04 [Tsyganenko, Sitnov, 2005]. The projection of the ground stations and the position of the satellites in the equatorial plane of the magnetosphere on February 15, 2011 at 07:00 UT are depicted in Figure 6. Distances between the stations in the magnetosphere were estimated in the XY plane; and from ground time delays, the signal propagation velocities V_{SCO_GHB}=68.1, V_{GHB_IQA}=21.2,

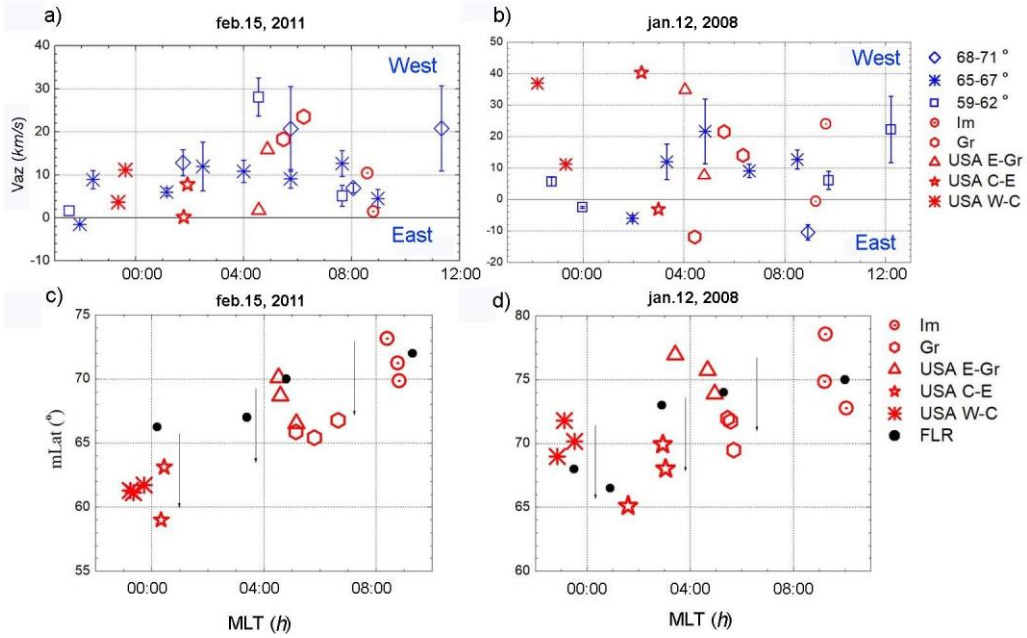

Figure 4. Distribution of azimuthal propagation velocities of geomagnetic pulsations and vortex centers of equivalent ionospheric currents relative to MLT (magnetic longitude) in the February 15, 2011 (*a*) and January 12, 2008 (*b*) events. Values are presented for 68°–71°, 65°–68°, 57°–60° latitude ranges. Positive velocities correspond to westward propagation; negative ones, to eastward propagation. Distribution is shown of the geomagnetic latitude of EIC vortices relative to MLT; black dots are the geomagnetic latitudes at which FLR oscillations were recorded in the same events on February 15, 2011 (*c*) and January 12, 2008 (*d*)

V_{IQA_FCC}=19.7 km/s. The obtained velocities are of the same order as the propagation velocities from satellite observations in the magnetosphere and match the maximum velocities from ground-based observations.

Figure 7 exhibits variations of the Umov—Poynting vector **S**=[**EH**] obtained by the ThE satellite in MFA (mean field aligned) coordinates. The field-aligned component is directed along the mean geomagnetic field, the azimuthal component is perpendicular to the magnetic meridian (positive in an easterly direction), the radial component is the vector product of the azimuthal component by the field-aligned one (positive direction toward higher L-shells): field-aligned — S_0 (*a*), azimuthal — S_a (*b*), radial — S_r (*c*) components; below in panels (*d*, *e*, *f*) are magnetic and electric field variations corresponding to these components, and phase shifts between them (*g*). In the S_0 component, the oscillation frequency is about 2 times higher than in the S_r component. The oscillation frequency in the S_a component at the beginning of the interval is about 2 times higher than at its end, the oscillations in this component are not as regular as in the S_0 component. Analysis of phase shifts shows that oscillations in the S_0 and S_r components are shifted by an angle of +/–200°; and in the S_a component, by 90°–100°, which corresponds to a standing wave under field line resonance. Different oscillation frequencies recorded by this satellite are also observed in measurements of plasma detectors, the oscillation frequency in the ion concentration (see Figure 1, *a*) is twice as high as that in their velocity (see Figure 1, *b*–*d*). Thus, waves of different types were simultaneously detected by this satellite.

Oliveira et al. [2020] address the question as to whether oscillations at fundamental and second harmonic frequencies can be simultaneously observed during field line resonance. The authors show that oscillations with different frequencies have different sources: oscillations with fundamental frequency are mainly excited by the interaction of interplanetary shock waves (ISW) with the magnetosphere, which do not have a tilt in the XZ plane; oscillations at the second harmonic frequency, by oblique ISW. Thus, we can hold that for the ThE satellite the oscillations with a multiple frequency are not different harmonics excited by resonance.

4. DISCUSSION

We have analyzed the azimuthal dynamics of Pc5 pulsations and their equivalent current systems in the magnetosphere and ionosphere in an extended longitude sector (0–12 MLT). We have found that vortex signatures in the magnetosphere propagate in the same direction as in the ionosphere, at velocities 5–10 times higher than the maximum azimuthal propagation velocity (25 km/s), as derived from ground-based observations. The velocities from ground-based and satellite observations are consistent with the results of other studies. In addition, our research has allowed us to identify some features, which are described below.

4.1. Dynamics of Pc5 geomagnetic pulsations and equivalent current vortices

The current system of Pc5 pulsations displayed in Figure 3, which represents Hall current vortices, allows them to be attributed to TCV events — isolated impulsive disturbances in the geomagnetic field consisting of two or more pulses of opposite polarity and observed on the dayside at high latitudes. As follows from Figures 3, 4, the vortices moved not only to the west, but also along the meridian, as well as to the east. The coincidence of

the propagation velocities of pulsations and vortices in magnitude and direction suggests that either the dynamics of vortices is the primary cause of pulsation propagation, or propagation of both vortices and pulsations has a common cause, for example, propagation of an MHD wave in the magnetosphere.

Azimuthal propagation from the nightside to the dayside can be explained as follows: Klibanova et al. [2016] has established that Pc5 pulsations mainly propagate from the dayside to the nightside, yet opposite propagation was also recorded. The authors attributed this to the excitation of oncoming waves due to reconnection in the nightside magnetosphere. In the present study, the events occurred under quiet conditions (there were no substorms), so we can assume that oncoming waves are excited due to reflection from the inner surface

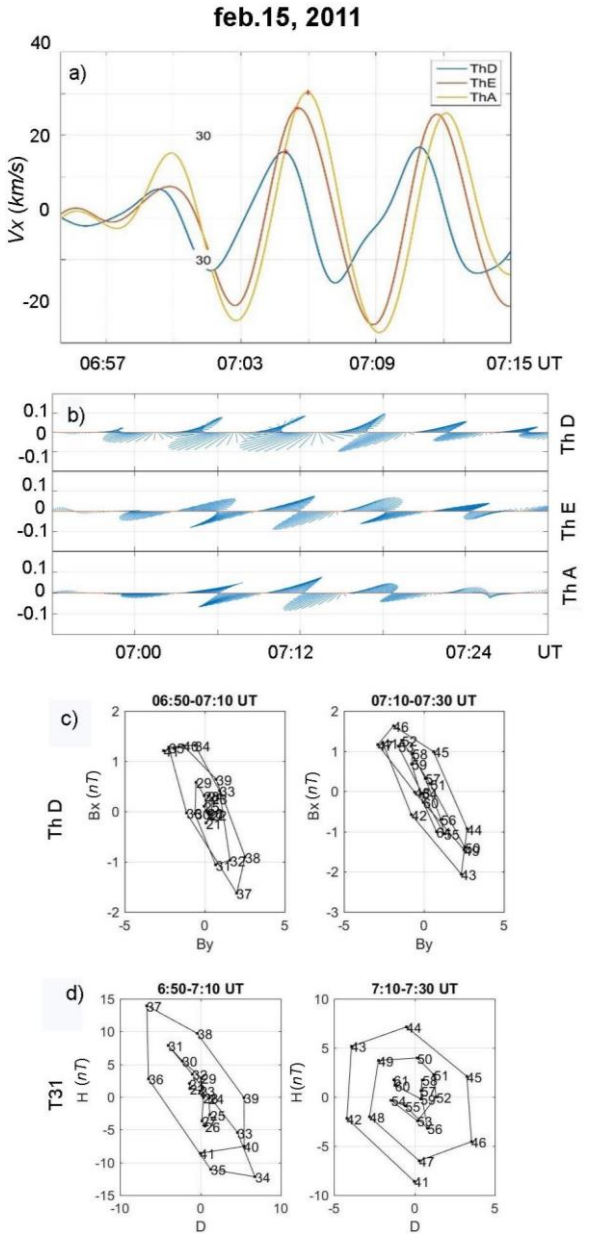

Figure 5. Variations in the ion velocity component *V* from satellites (Th D, E, A) (*a*), magnetic field hodographs from satellites (*b*), magnetic field polarization from the ThD satellite (*c*), magnetic field polarization from ground station T31 (*d*). The data is filtered in the Pc5 range

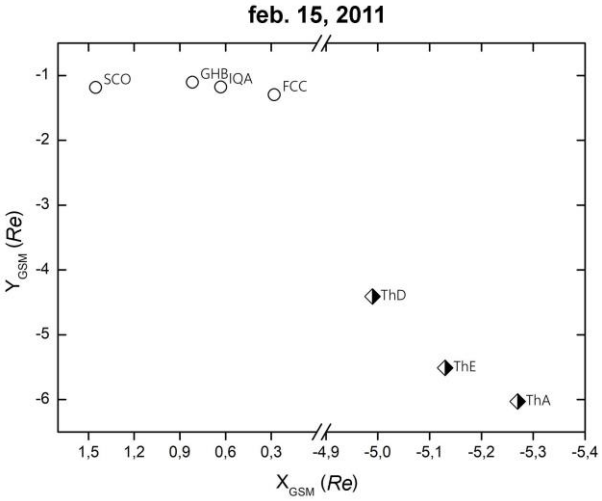

Figure 6. Projection of ground stations located along 68°–71° magnetic latitudes (circles) and position of satellites (diamonds) in the equatorial plane of the magnetosphere on February 15, 2011 at 07:00 UT

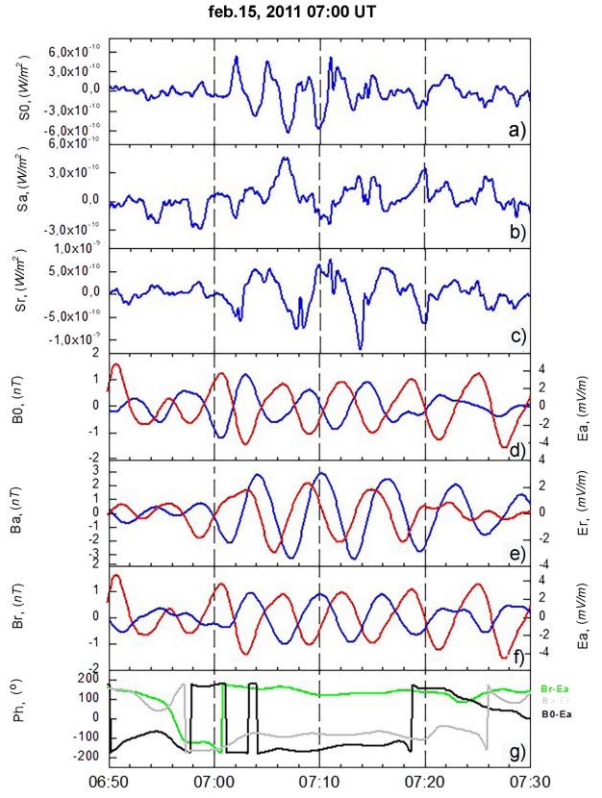

Figure 7. Variations in the Umov—Poynting vector recorded by the ThE satellite: field-aligned (*a*), azimuthal (*b*), radial (*c*) components, field-aligned (*d*), azimuthal (*e*), radial (*f*) components of the magnetic field, and azimuthal and radial components of the electric field from the ThE satellite, and phase shifts between them. In panels *d*, *e*, *f*, the magnetic field is marked in blue; and the electric field, in red

of the resonator, in which pulsations are generated. Note that the existence of such a resonator was reported in [Mazur, Leonovich, 2006].

This study allows us to compare phase velocities of pulsation propagation and group velocities of vortex propagation: analysis of Figure 4 *a*, *b* shows that these velocities are close. If in the February 15, 2011 event the

vortex velocities were close to zero (see Figure 5, *a*), in the January 12, 2008 event they mostly exceeded the pulsation velocities.

4.2. Magnetospheric projection of vortices of equivalent ionospheric currents

Zesta et al. [2002] have observed that TCVs have resonance characteristics. At the same time, Figure 4 *c*, *d* indicates that geomagnetic latitudes of EIC vortices coincide with the latitudes at which FLRs occurred. Thus, the results of this work on the agreement between positions of vortices and field line resonances are confirmed by earlier studies.

Figure 4 *c*, *d* also shows that latitudes of vortices and field line resonances decreased to earlier MLT. The displacement of vortices to lower latitudes is probably due to the fact that resonance oscillations occur at higher frequencies and hence on shorter field lines. Variations in resonance oscillation frequencies are probably caused by significant spatial variations in the geomagnetic field strength modulus in the region where vortices were detected, as shown in the IGRF-13 model [Alken et al., 2021].

The magnetospheric location of the vortices in both events considered corresponds to the plasma sheet (see position of satellites in Table 3) and is projected onto closed field lines. Comparison of the vortex latitudes in Figure 4 *c*, *d* with the results of MHD modeling obtained in [Maffei et al., 2023] also shows that the vortex latitudes are located south of the boundary of closed and open field lines. Projection of vortices on closed lines is consistent with the results received in [Yahnin, Moretto, 1996], in which the authors found that the projection of vortices, presumably having a source located in SW, turned out to be deep in the magnetosphere. We can assume that vortices in the plasma sheet arise due to an indirect effect — generation of shear flows [Kakad et al., 2003], which accompanies a resonance phenomenon in the magnetosphere.

4.3. Simultaneous detection of fast magnetosonic and Alfvén waves

Observation of oscillations of different frequencies by one satellite, as in the February 15, 2011 event (see Figures 1, 6), has been described by Korotova et al. [2020]; the authors interpreted them as compression mode oscillations (field-aligned oscillations) recorded near the geomagnetic equator. At the same time, oscillations with twice the period were interpreted as transverse oscillations.

In the February 15, 2011 event, the ThE satellite was in the equatorial plane and simultaneously recorded a fast magnetosonic wave in the field-aligned component of the Umov—Poynting vector (see Figure 7, *a*) and in the ion concentration (Figure 1, *a*), as well as an Alfvén wave in the azimuthal, radial components (Figure 7, *b*), and in velocity variations (see Figure 1, *b*–*d*), which carried the field-aligned current. The vortices we observe are likely to correspond to the ionospheric footpoints of these field-aligned currents.

CONCLUSION

From the analysis we can draw the following conclusions. Vortex signatures in the magnetosphere propagate in the same direction as in the ionosphere at velocities 5–10 times higher than the maximum azimuthal propagation velocity (25 km/s), as derived from ground-based observations. We have established that the phase velocities of propagation of Pc5 geomagnetic pulsations coincide in magnitude and direction with the group velocities of vortices in the events considered. The geomagnetic latitudes of EIC vortices are shown to match the latitudes at which field line resonances were observed. These latitudes decrease toward earlier MLT.

Taking into account that azimuthal propagation of pulsations and vortices occurs both from the dayside to the nightside and in the opposite direction, we believe that the observed dynamics reflects the behavior of MHD wave propagation in the magnetosphere.

We thank leaders of the following projects for providing access to data: the SUPERMAG project, including the IMAGE network, (PI Liisa Juusola), GREENLAND COAST CHAIN data, (PI Anna N. Willer), Themis, CANMOS, Geomagnetism Unit of the Geological Survey of Canada; GIMA; Intermagnet; USGS, as well as satellite observation dataset from CDAWEB (D.J. McComas, R. Lepping, K. Ogilvi, G. Paschmann).

The work was financially supported by the Ministry of Science and Higher Education of the Russian Federation.

REFERENCES

Alken P., Thébault E., Beggan C.D., Amit H., Aubert Baerenzung, J. Bondar T.N., et al. International Geomagnetic Reference Field: the thirteenth generation. *Earth Planets Space*. 2021, vol. 73, no. 49. DOI: 10.1186/s40623-020-01288-x.

Allan W., White S.P., Poulter E.M. Impulse-excited hydromagnetic cavity and field-line resonances in the magnetosphere. *Planet. Space Sci*. 1986, vol. 34, pp. 371–385. DOI: 10.1016/0032-0633(86)90144-3.

Amm O., Engebretson M.J., Hughes T., Newitt L., Viljanen A., Watermann J. A traveling convection vortex event study: Instantaneous ionospheric equivalent currents estimation of field-aligned currents and the role of induced currents. *J. Geophys. Res*. 2002, vol. 107, no. A11, p. 1334. DOI: 10.1029/2002JA009472.

Chelpanov M.A., Anfinogentov S.A., Kostarev D.V., Mikhailova O.S., Rubtsov A.V., Fedenev V.V., Chelpanov A.A. Review and comparison of MHD wave characteristics at the Sun and in Earth's magnetosphere. *Solar-Terr. Phys*. 2022, vol. 8, iss. 4, pp. 3–27. DOI: 10.12737/stp-84202201.

Chen L., Hasegawa A. A theory of long-period magnetic pulsations: 1. Steady state excitation of field line resonance. *J. Geophys. Res.* 1974, vol. 79, no. 7, pp. 1024–1032. DOI: 10.1029/JA079i007p01024.

Chinkin V.E., Soloviev A.A., Pilipenko V.A. Identification of Vortex Currents in the Ionosphere and Estimation of Their Parameters Based on Ground Magnetic Data. *Geomagnetism and Aeronomy*. 2020, vol. 60, no. 5. pp. 559–569. DOI: 10.1134/S0016793220050035.

Dmitriev A.V., Suvorova A.V. Atmospheric Effects of Magnetosheath. *Jets. Atmosphere*. 2023, vol. 14, iss. 1, p. 45. DOI: 10.3390/atmos14010045.

Friis-Christensen E.S., McHenry M.A., Clauer C.R., Vennerstrøm S. Ionospheric traveling convection vortices observed near the polar cleft-A triggered response to sudden changes in the solar wind. *Geophys. Res. Lett.* 1988, vol. 15, iss.3, pp. 253–256. DOI: 10.1029/GL015i003p00253.

Gjerloev J.W. The SuperMAG data processing technique. *J. Geophys. Res.* 2012, vol. 117, no. A09213. DOI: 10.1029/2012JA017683.

Glassmeier K.-H. Traveling magnetospheric convection twin-vortices: Observations and theory. *Ann. Geophys*. 1992, vol. 10, p. 547.

Glassmeier K.-H., Othmer C., Gramm R., Stellmacher M., Engebretson M. Magnetospheric field-line resonances: A comparative planetology approach. *Earth Environment Sci*. 1999, vol. 20, pp. 61–109.

Hemming R.V. Digital filters. M.: Sov.radio. 1980, 224 p. (In Russian).

Kakad A.P., Lakhina G.S., Singh S.V. A shear flow instability in plasma sheet region. *Planet Space Sci*. 2003, vol. 51, p. 177.

Klibanova Y.Y., Mishin V.V., Tsegmed B., Moiseev A.V. Properties of daytime long-period pulsations during magnetospheric storm commencement. *Geomagnetism and Aeronomy*. 2016, vol. 56, no. 4, pp. 426–440. DOI: 10.1134/S0016793216040071.

Korotova G.I., Sibeck D.G., Singer H.J., Rosenberg T.J., Engebretson M.J. Interplanetary magnetic field control of dayside transient event occurrence and motion in the ionosphere and magnetosphere. *Ann. Geophys*. 2004, vol. 22, pp. 4197–4202.

Korotova G., Sibeck D., Engebretson M., Balikhin M., Thaller S., Kletzing C. Spence H., Redmon R. Multipoint observations of compressional Pc5 pulsations in the dayside magnetosphere and corresponding particle signatures. *Ann. Geophys*. 2020, vol. 38, pp. 1267–1281. DOI: 10.5194/angeo-38-1267-2020.

Lühr H.M., Lockwood P.E., Sandholt T.L., Hansen T. Multi-instrument ground-based observations of a travelling convection vortices event. *Ann. Geophys*. 1996, vol. 14, no. 2, pp. 162–181.

Maffei S., Eggington J.W.B., Livermore P.W., Mound J.E., Sanchez S., Eastwood J.P., Freeman M.P. Climatological predictions of the auroral zone locations driven by moderate and severe space weather events. *Scientific Rep*. 2023, vol. 13, p. 779. DOI: 10.1038/s41598-022-25704-2.

Makarov G.A., Solovyev S.I., Engebretson M., Yumoto K. Azimuth propagation of geomagnetic sudden pulse in high latitudes at the December 15, 1995 sharp decrease in a solar wind density. *Geomagnetizm i aeronomiya* [Geomagnetism and Aeronomy]. 2002, vol. 42, no.1, pp. 42–50. (In Russian).

Mann I.R., Voronkov I., Dunlop M., Donovan E., Yeoman T.K., Milling D.K., Wild J., Kauristie K., Amm O., Bale S.D., Balogh A., Viljanen A., Opgenoorth H.J. Coordinated ground-based and Cluster observations of large amplitude global magnetospheric oscillations during a fast solar wind speed interval. *Ann. Geophys*. 2002, vol. 20, pp. 405–426. DOI: 10.5194/angeo-20-405-2002.

Mazur V.A., Leonovich A.S. ULF hydromagnetic oscillations with the discrete spectrum as eigenmodels of MHD-resonator in the near-Earth part of the plasma sheet. *Ann. Geophys*. 2006, vol. 24, no. 6, pp. 1639–1648.

Mishin V.V., Matiukhin Iu.G. Kelvin-Helmholtz instability in the magnetopause as a possible source of wave energy in the Earth's magnetosphere. *Geomagnetizm i Aeronomiia*. 1986, vol. 26, pp. 952–957. (In Russian).

Motoba T., Kikuchi T., Lühr H., Tachihara H., Kitamura T.I., Hayash K. Global Pc5 caused by a DP2-type ionospheric current system. *J. Geophys. Res*. 2002, vol. 107, pp. 1032–1047. DOI: 10.1029/2001JA900156.

Oliveira D.M., Hartinger M.D., Xu Z., Zesta E., Pilipenko V.A., Giles B.L., Silveira M.V.D. Interplanetary shock impact angles control magnetospheric ULF wave activity: Wave amplitude, frequency, and power spectra. *Geophys. Res. Lett*. 2020, vol. 47, pp. 1–11. DOI: 10.1029/2020GL090857.

Saito T. Geomagnetic pulsations. *Space Sci. Rev*. 1969, vol. 10, iss. 3, pp. 319–412.

Saito T. Long-period irregular magnetic pulsation Pi3. *Space Sci. Rev*. 1978, vol. 21, pp. 427–467. DOI: 10.1007/BF00173068.

Southwood D.J. Some features of field line resonances in the magnetosphere. *Planet. Space Sci*. 1974, vol. 22, pp. 483–491.

Tsyganenko N.A., Sitnov M.I. Modeling the dynamics of the inner magnetosphere during strong geomagnetic storms. *J. Geophys. Res*. 2005, vol. 110, A03208. DOI: 10.1029/2004JA010798.

Vanhamäki H., Juusola L. Introduction to Spherical Elementary Current Systems. *Ionospheric Multi-Spacecraft Analysis Tools*. 2020, vol. 17, pp. 5–33. DOI: 10.1007/978-3-030-26732-2_13.

Wright A.N. Dispersion and wave coupling in inhomogeneous MHD waveguides. *J. Geophys. Res*. 1994, vol. 99, pp. 159–167. DOI: 10.1029/93JA02206.

Yahnin A., Moretto T. Travelling convection vortices in the ionosphere map to the central plasma sheet. *Ann. Geophys*. 1996, vol. 14, pp. 1025–1031. DOI: 10.1007/s00585-996-1025-3.

Zhang W., Nishimura Y., Wang B., Hwang K.-J., Hartinger M. D., Donovan E. F. Identifying the structure and propagation of dawnside Pc5 ULF waves using space-ground conjunctions. *J. Geophys. Res.: Space Phys*. 2022, vol. 127, no. 12, p. e2022JA030473. DOI: 10.1029 2022JA030473.

Zesta E., Hughes W.J., Engebretson M.J. A statistical study of traveling convection vortices using the Magnetometer Array for Cusp and Cleft Studies. *J. Geophys. Res*. 2002, vol. 107, pp. 18.1–18.21. DOI: 10.1029/1999JA000386.

URL: http://supermag.jhuapl.edu/mag (accessed March 22, 2024).

URL: http://cdaweb.gsfc.nasa.gov (accessed March 22, 2024).

URL: https://link.springer.com/chapter/10.1007/978-3-030-26732-2_2#Sec18 (accessed March 22, 2024).

URL: https://www.mathworks.com/help/signal/ref/findpeaks.html (accessed March 22, 2024).

This paper is based on material presented at the 19th Annual Conference on Plasma Physics in the Solar System, February 5–9, 2024, IKI RAS, Moscow.

Original Russian version: Moiseev A.V., Popov V.I., Starodubtsev S.A., published in Solnechno-zemnaya fizika. 2024. Vol. 10. No. 3. P. 104–115. DOI: 10.12737/szf-103202412. © 2024 INFRA-M Academic Publishing House (Nauchno-Izdatelskii Tsentr INFRA-M)

How to cite this article

Moiseev A.V., Popov V.I., Starodubtsev S.A. Investigating azimuthal propagation of Pc5 geomagnetic pulsations and their equivalent current vortices from ground-based and satellite data. *Solar-Terrestrial Physics*. 2024. Vol. 10. Iss. 3. P. 97–107. DOI: 10.12737/stp-103202412.